

Article

Comparative Performance of Aerial RGB vs. Ground Hyperspectral Indices for Evaluating Water and Nitrogen Status in Sweet Maize

Milica Colovic ¹, Anna Maria Stellacci ^{2,*}, Nada Mzid ^{3,4,*}, Martina Di Venosa ², Mladen Todorovic ⁵, Vito Cantore ⁶ and Rossella Albrizio ⁷

¹ Istituto Nazionale di Fisica Nucleare, Sezione di Bari, 70125 Bari, Italy; milica.colovic@ba.infn.it

² Department of Soil, Plant and Food Sciences, University of Bari Aldo Moro, Via G. Amendola 165/a, 70126 Bari, Italy; m.divenosa3@studenti.uniba.it

³ Interdepartmental Research Centre on the “Earth Critical Zone”, Università degli Studi di Napoli Federico II, Via Università 100, Portici, 80055 Naples, Italy

⁴ Department of Agriculture, Università degli Studi di Napoli Federico II, Via Università 100, Portici, 80055 Naples, Italy

⁵ CIHEAM—Mediterranean Agronomic Institute of Bari, 70010 Valenzano, Italy; mladen@iamb.it

⁶ Institute of Sciences of Food Production (ISPA), National Research Council (CNR), Via Amendola, 122/O, 70125 Bari, Italy; vito.cantore@ispa.cnr.it

⁷ Institute for Mediterranean Agricultural and Forestry Systems, National Research Council of Italy, P. le Enrico Fermi 1, 80055 Portici, Italy; rossella.albrizio@cnr.it

* Correspondence: annamaria.stellacci@uniba.it (A.M.S.); nada.mzid@unina.it (N.M.)

Abstract: This study analyzed the capability of aerial RGB (red-green-blue) and hyperspectral-derived vegetation indices to assess the response of sweet maize (*Zea mays* var. *saccharata* L.) to different water and nitrogen inputs. A field experiment was carried out during 2020 by using both remote RGB images and ground hyperspectral sensor data. Physiological parameters (i.e., leaf area index, relative water content, leaf chlorophyll content index, and gas exchange parameters) were measured. Correlation and multivariate data analysis (principal component analysis and stepwise linear regression) were performed to assess the strength of the relationships between eco-physiological measured variables and both RGB indices and hyperspectral data. The results revealed that the red-edge indices including $CI_{red-edge}$, NDRE and DD were the best predictors of the maize physiological traits. In addition, stepwise linear regression highlighted the importance of both WI and WI:NDVI for prediction of relative water content and crop temperature. Among the RGB indices, the green-area index showed a significant contribution in the prediction of leaf area index, stomatal conductance, leaf transpiration and relative water content. Moreover, the coefficients of correlation between studied crop variables and GGA, ND_{Luv} and ND_{Lab} were higher than with the hyperspectral indices measured at the ground level. The findings confirmed the capacity of selected RGB and hyperspectral indices to evaluate the water and nitrogen status of sweet maize and provided opportunity to expand experimentation on other crops, diverse pedo-climatic conditions and management practices. Hence, the aerially collected RGB vegetation indices might represent a cost-effective solution for crop status assessment.

Keywords: *Zea mays* L.; red-green-blue indices; hyperspectral sensors; UAV; red-edge region; water and nitrogen stresses



Citation: Colovic, M.; Stellacci, A.M.; Mzid, N.; Di Venosa, M.; Todorovic, M.; Cantore, V.; Albrizio, R. Comparative Performance of Aerial RGB vs. Ground Hyperspectral Indices for Evaluating Water and Nitrogen Status in Sweet Maize. *Agronomy* **2024**, *14*, 562. <https://doi.org/10.3390/agronomy14030562>

Academic Editors: Sara Álvarez and Sergio Vélez

Received: 25 January 2024

Revised: 6 March 2024

Accepted: 7 March 2024

Published: 11 March 2024



Copyright: © 2024 by the authors. Licensee MDPI, Basel, Switzerland. This article is an open access article distributed under the terms and conditions of the Creative Commons Attribution (CC BY) license (<https://creativecommons.org/licenses/by/4.0/>).

1. Introduction

Nowadays, food security is challenged by a continuous growth of population, which would trigger an increase in food demand in 2050 by more than 70% relative to the beginning of the century [1]. Hence, agricultural production has been intensified in many areas causing serious environmental burden and economic consequences [2]. The intensification

of cultivation is associated with reduced availability and quality of natural resources, such as water and land, which imposes a need to adopt sustainable management techniques and preserve resources for future generations [2].

Precision agriculture represents a suitable strategy to respond to dynamic and spatially different crop demands, and to implement integrated land, soil, water, nutrient and crop management approaches. In this context, remote- and proximal-sensing tools have proven to be widely efficient for detection and management of water stress and nutrient deficiency at field level [3,4] and across the large-scale regions [5]. Policymakers, stakeholders, and end-users highlighted the importance of sensing technologies in assisting farmers to adopt sustainable agricultural practices, optimize irrigation and nutrient inputs and achieve profitable yields [6].

Remote and proximal sensors detect electromagnetic wave reflectance information from canopies related to numerous crop parameters [7]. Vegetation reflectance properties depend on morphological and chemical characteristics of the leaf surface [8]. Leaf structure, water content, nutritional status, disease, pigmentation, phyllotaxis, sun exposition and phenological stage are some of many factors that affect plant spectral reflectance [9]. A very high reflectance in the near-infrared region (NIR, 760–900 nm), high in the green region (520–570 nm), and low in blue (400–500 nm) and red (630–690 nm) regions are typically observed for plants grown under optimal conditions [10]. In the visible region (VIS, 400–700 nm), vegetation reflectance is strongly affected by pigments within the leaves [11]. Otherwise, the reflectance of NIR radiation depends on the internal structure of leaves, cells, and tissues [12]. Spectral reflectance in the short-wave infrared region (SWIR, 1300–2500 nm) is affected by water content in plant tissues [12]. Reduced water content implies reduced reflectance in the SWIR region [13]. Bands at around 970, 1200, 1400, and 1900 nm can be useful for estimating vegetation water content in the NIR and SWIR regions [14,15].

Various studies [10,16] have proven the possibility of using hyperspectral data to assess nitrogen (N) and water status of crops. The principle behind hyperspectral sensing studies for N status assessment is the relationship between chlorophyll and nitrogen [17]. In the case of N deficiency, the visible, the red-edge and the NIR regions provide valuable information for computing vegetation indices [10,16]. The red-edge position is obtained by the point of maximum slope between the red chlorophyll absorption region and the region of high NIR reflectance [18]. The shape and position of the red-edge are affected by changes in chlorophyll content and thus by changes in vegetation nitrogen content [16]. Among the chlorophyll vegetation indices, the green chlorophyll index (CI_{green}) accurately estimated N content in maize; also, the red-edge chlorophyll index ($CI_{red-edge}$), with the red-edge band between 720–740 nm, was found optimal for the same goal [19].

The high potential of using hyperspectral technologies to assess water status is also confirmed by studies conducted on several plant species such as wheat, tomato, soybean, potato and maize [20–25]. The water index (WI; [26]), the moisture stress index (MSI; [27]), the normalized water index (NWI; [28]) and the simple ratio water index (SRWI; [29]) are some of the hyperspectral vegetation indices involved in monitoring crop water content and water stress. Despite these numerous studies, the selection of the most suitable vegetation indices for crop water status assessment remains questionable, due to the high variety of crops and different growing conditions.

Several studies proved the suitability of portable spectroradiometers to estimate physiological vegetation properties. However, this approach presents limitations related to the portability, the time required to collect measurements, the punctual data acquisition and the high cost [30,31].

In this regard, the use of RGB (red-green-blue) images obtained by digital camera placed on unmanned aerial vehicle (UAV) platforms is particularly suitable for the monitoring of sparsely grown annual crops (e.g., sweet maize) in arid and semi-arid Mediterranean regions where irrigation and fertilization are often not well regulated in terms of time and quantity [32]. The use of RGB images above the canopy provided accurate results in differ-

ent application fields related to agriculture and biology [33]. Generally, the RGB imaging method has been developed for rapid and non-invasive determination of color changes caused by nutritional stress such as chlorophyll content deficiency in plant leaves [34]. Based on this principle, the detection of leaf color changes can be used to monitor the progress of water and nutritional stress, and plant diseases and senescence. Furthermore, the use of information collected from digital RGB photos for calculating vegetation indices provides a low-cost alternative to multispectral and hyperspectral data [35]. Advances in digital photography would be a viable and economical monitoring option for precision agriculture [36].

Numerous studies confirmed the utility of vegetation indices computed from RGB imaging to detect plant performance under a variety of conditions at both canopy and leaf scale [37–40]. Purcell et al. [41] have reported that digital-image analysis is a simple method providing an assessment of maize nitrogen status with the potentiality to diagnose crop needs. Gracia-Romero et al. [42], in a study on maize under phosphorus fertilization, compared vegetation indices detected by aerial and ground-based RGB and aerial multispectral sensors. They showed that ground-measured RGB indices (such as hue, a^* , u^* , GA and GGA indices) were significantly affected by the absence of fertilizer and they had better performance in predicting grain yield than multispectral indices. In a study performed on wheat under different irrigation regimes, the vegetation indices obtained from RGB images showed a similar or slightly better performance than NDVI in predicting yield [43]. According to [44], RGB indices can be successfully employed at canopy and leaf level for the management of wheat and maize growth under different fertilizers and irrigation regimes, for disease monitoring, and as an effective high-throughput phenotyping technique in breeding programs. RGB images can be processed by analyzing red-, green-, and blue-light broadband reflectance values or by employing different color spaces, such as the Breedpix code [42]. In this sense, the RGB technique is revealed to be a powerful and low-cost methodology for evaluating crop performance.

There is evidence from the literature about the high number of studies concerning the use of spectral indices to independently evaluate nitrogen and water status of crops, utilizing either RGB or hyperspectral indices [20,39,45]. However, to the best of our knowledge, none of these studies have specifically addressed the assessment of maize crop response under varied water and nitrogen conditions by integrating both sensing techniques simultaneously.

Therefore, the objective of our study was to compare the performance of aerially collected RGB indices and ground-measured hyperspectral data in the estimation of eco-physiological variables of sweet maize grown under different water and nitrogen regimes.

2. Materials and Methods

2.1. Study Area and Growing Conditions

Field trials were carried out at the experimental field of the Mediterranean Agronomic Institute (IAMB) in Valenzano, Bari (41°03' N, 16°53' E, 77 m above sea level), Southern Italy, during the 2020 growing season. The area experiences typical Mediterranean weather, with mild winters and dry summers. The soil in the study region is silty clay loam. The average values of the main physical and chemical soil properties are: sand 170 g kg⁻¹, clay 234 g kg⁻¹, silt 596 g kg⁻¹, USDA Textural Class: silty loam; pH (H₂O 1:2.5) 8.1, electrical conductivity (1:2) 0.24 dS m⁻¹, total carbonate 55 g kg⁻¹, organic C 11.6 g kg⁻¹, total N 0.9 g kg⁻¹, C/N ratio 12.9, available P 17 mg kg⁻¹, exchangeable K 465 mg kg⁻¹.

From June to September 2020, sweet maize (*Zea mays* var. *saccharata* L., hybrid Centurion F1) was cultivated in rows 0.5 m apart, with a plant density of 10 plants m⁻², in 18 plots (10 × 10 m). Sweet maize was grown under three water treatments: full irrigation (I100), deficit irrigation (I50) and rainfed (I0), and two nitrogen levels: high nitrogen (HN—300 kg ha⁻¹) and low nitrogen (LN—50 kg ha⁻¹).

A split-plot experimental design with three replicates was used to allocate the treatments, with water regime (WR) as the main plot factor and nitrogen (N) as the sub-plot factor.

Agro-meteorological data (air temperature, relative humidity, solar radiation, wind speed, and precipitation) were collected daily from the weather station near the experimental field.

The drip irrigation method was used to supply water to irrigated treatments. Irrigation scheduling was managed by using an Excel-model, based on the FAO standard approach [46], which calculates crop evapotranspiration and irrigation water requirements on a daily basis. A seasonal irrigation amount of 291 mm was supplied to I100 treatment, while half of that amount was given to I50.

2.2. Crop Physiological Data Collection

Gas exchanges in terms of CO₂ net assimilation rate (A_n , $\mu\text{mol m}^{-2} \text{s}^{-1}$), stomatal conductance (g_s , $\text{mol m}^{-2} \text{s}^{-1}$), and leaf transpiration (T_r , $\text{mmol m}^{-2} \text{s}^{-1}$) were measured with a portable open-system gas-exchange analyzer (Li-6400XT, Li-Cor Biosciences, Lincoln, NE, USA). The measurements were taken on well-exposed, healthy and intact leaves, over a clipped leaf surface of 6.0 cm², and were replicated three times per plot.

The chlorophyll content index (CCI), which is related to leaf greenness was assessed with an optical meter (SPAD-502, Konica Minolta, Osaka, Japan), on 25 replicates per plot.

Relative water content (RWC) was measured in leaves like those used for gas exchange measurements. At midday, nine leaf segments were cut from three plants in each plot. RWC was calculated as the ratio of the difference between the fresh weight (FW) of the leaf segments and their dry weight (DW) to the difference between the fresh weight and saturated weight (SW).

Canopy temperature (T_c) was measured with a thermal imaging camera (FLIR B335, Wilsonville, OR, USA) with a resolution of 640-by-480 pixels and a thermal sensitivity higher than 0.1 °C. the FLIR Tools software (version 9.4.5) for leaf temperature extraction was used to elaborate the images. T_c measurements were replicated three times per plot.

Leaf area index (LAI) was assessed using an optical leaf area meter (Li-COR, 3100, Lincoln NE, USA). Then, dry-above-ground biomass (DAGB) was measured on the same samples used for LAI by weighing them after drying in the oven at 70 °C for 48 h. Both LAI and DAGB measurements were replicated three times per plot.

All the above-mentioned measurements were performed 5 times during the crop cycle from 13th of July until the end of August.

2.3. RGB Image Acquisition and Analysis

RGB images were collected using the digital camera installed on a drone (Mavik 2 PRO, DJI, Shenzhen, China). Each image was taken holding the drone at 80–100 cm above the canopy level, in the zenithal plane (Figure 1). The acquisition of images was carried out from the development stage until the harvesting on sunny days and it was replicated three times for each plot.

The Breedpix 0.2 program, modified for JAVA 8 and included as a plugin in FIJI (<https://github.com/George-haddad/CIMMYT>, accessed on 24 January 2024), was used to analyze RGB images. This program allows for the extraction of RGB specific vegetation indices (VIs) in connection to various color characteristics [43]. Utilizing BreedPix functions, RGB values were changed to hue-saturation-intensity (HSI) values, which are based on natural color visualization. Chromatic coordinates from the CIELab and CIELuv color spaces were simultaneously determined, as in [47].

Hence, several indices (Table 1) were calculated using either the average color of the entire image in various units related to “greenness” or the proportion of pixels classified as green canopy relative to the total number of pixels in the image. The hue (H) component of the HSI color space describes the color spanning the visible spectrum in the form of an angle between 0° and 360°, where 0° corresponds to red, 60° to yellow, 120° to green, and 180° to cyan [39].

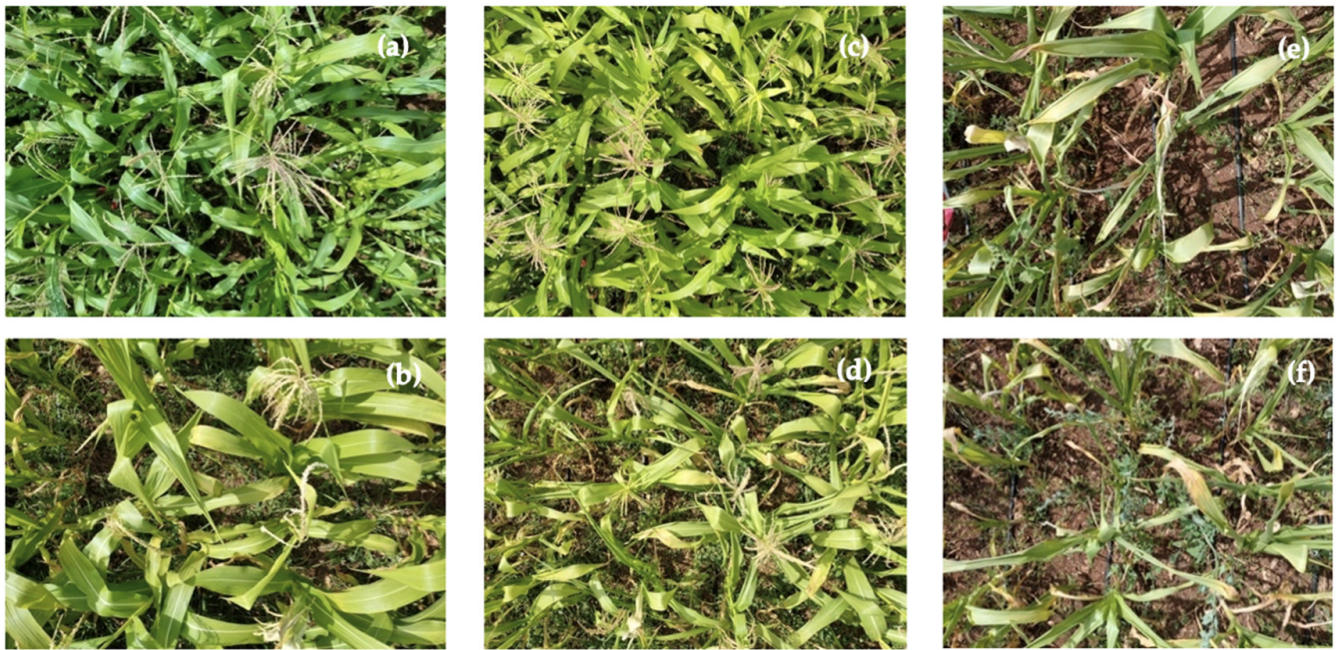


Figure 1. RGB images taken during the flowering season over six different treatments: I100 HN (a), I100 LN (b), I50 HN (c), I50 LN (d), I0 HN (e), I0 LN (f).

Table 1. Indices derived from RGB images.

Index	Formula	Color Model
Hue (H)	Hue < 0°	HIS color model
	Hue < 60°	HIS color model
	Hue < 120°	HIS color model
	Hue < 180°	HIS color model
Green Area (GA)	60° < Hue < 180°	HIS color model
Greener Area (GGA)	80° < Hue < 180°	HIS color model
a*	green—red	CIELab color model
b*	blue—yellow	CIELab color model
u*	blue—green (v*)—red (u*)	CIEluv color model
v*		CIEluv color model
NDLab	$((1 - a^*) - b^*) / ((1 - a^*) + b^*) + 1$	CIELab color model
NDLuv	$((1 - u^*) - v^*) / ((1 - u^*) + v^*) + 1$	CIEluv color model

Green area index (GA) is the percentage of pixels with $60 < \text{Hue} < 120$ from the total amount of pixels, whereas the greener area (GGA) is a little more limiting, since the index corresponds to $80 < \text{Hue} < 120$, excluding yellowish-green tones. Moreover, GGA is proposed to capture the active photosynthetic area excluding senescent leaves.

In the CIELab color space model, the L^* dimension denotes lightness, while the a^* -component represents the green-to-red range, with a greater positive value signifying a purer red and a lower positive value indicating a greener hue. Meanwhile, the b^* component expresses the transition from blue to yellow, with the more positive value being closer to pure yellow and the more negative value being closer to blue. In the CIEluv color space model, dimensions u^* and v^* are perceptually uniform coordinates, where L^* is again lightness and u^* and v^* represent the axes, like a^* and b^* , separating the color spectrum, respectively.

Furthermore, both CIELab and CIEluv include color calibration corrections by separating the color hue from the illumination elements of the input RGB signal. For that reason,

as was proposed by [39], we used two vegetation indices based on these color spaces, computing the normalized difference between a^* and b^* (NDLab) and the normalized difference between u^* and v^* (NDLuv) in a manner similar to the conceptual basis of NDVI.

As a result, the CIELab and CIELuv color spaces may contrast green vegetation abundance with both the reddish/brown soil background (fractional vegetation cover or plant growth) and the yellowing induced by chlorosis (loss of foliar chlorophyll), both of which are typical indications of nitrogen deficit.

2.4. Hyperspectral Reflectance Acquisition and Analysis

Plant reflectance, with wavelength range of 325–1075 nm, accuracy of ± 1 nm, and resolution lower than 3 nm at 700 nm, was measured by using a high-spectral-resolution ASD FieldSpec Hand-Held 2 spectroradiometer (Analytical Spectral Devices, Inc., Boulder, CO, USA). The field of view (FOV) of the bare fiber-optic probe was 25° . The spectrum of a white (BaSO₄) reference panel with known reflectance properties was acquired to derive the reflectance of the target.

The vegetation spectrum was measured 10 cm above the canopy (spot size of about 14 cm²). Measurements were acquired from three plants per plot.

Data were processed by means of View Spec software (version 6.0). Vegetation indices (Table 2) were calculated using different spectral bands.

Table 2. The indices derived from the hyperspectral visible and near-infrared bands used in this study.

Acronym	Index	Equation	Reference
CI		$(R_{880}/R_{590}) - 1$	
CI _{green}	Chlorophyll indices	$(R_{730}/R_{530}) - 1$	[48]
CI _{red-edge}		$(R_{850}/R_{730}) - 1$	
MTCI		$(R_{760} - R_{720})/(R_{720} - R_{670})$	
DD	Double difference index	$(R_{749} - R_{720}) - (R_{701} - R_{672})$	[16]
REIP	Red-edge inflection point	$700 + 40 \times [(((R_{670} + R_{780})/2) - R_{700})/(R_{740} - R_{700})]$	[49]
NDRE	Normalized difference red-edge	$(R_{790} - R_{720})/(R_{790} + R_{720})$	[50]
WI	Water band index	R_{970}/R_{900}	[26]
WI:NDVI	Ratio of water band index and normalized difference vegetation index	$(R_{970}/R_{900})/[(R_{800} - R_{680})/(R_{800} + R_{680})]$	[26]

2.5. Statistical Analysis

Data were statistically analyzed using the software R Studio (4.0.2, 2018; R Foundation for Statistical Computing, Vienna, Austria). Normal distribution and homogeneity of variance were preliminarily checked. A two-factor analysis of variance considering a split-plot experimental design (with WR as the main plot factor and N as the sub-plot factor) was applied to investigate the impact of growing conditions (water treatments and nitrogen levels) and their interaction on physiological parameters at the tasseling stage. Fisher's LSD (least significant difference) test was used to identify post hoc differences at each growing condition.

Bivariate Pearson correlation coefficients were computed on the data collected over the whole growing season ($n = 270$), to examine the correlations between the physiological parameters, RGB indices and hyperspectral vegetation indices. On the same data set, the multiple linear regressions were calculated using a stepwise algorithm with physiological parameters as dependent variables and RGB and hyperspectral vegetation indices as independent variables. Principal component analysis (PCA) was computed to explore the relationship between RGB and hyperspectral vegetation indices. PCA was computed on the standardized variables. The PCs that explained a significant part of the total

variance were selected and within each selected PC the loadings of the original variables were examined.

3. Results

At the tasseling stage, water regimes significantly affected all physiological variables (LAI, CCI, gas exchange parameters and RWC), while nitrogen had a significant impact only on CCI. The interaction between water and nitrogen was significant only for CCI, as shown in Table 3.

Table 3. Effect of water regime and nitrogen level on leaf area index (LAI), chlorophyll content index (CCI), net assimilation rate (A_n), stomatal conductance (g_s) and relative water content (RWC) measured at VT (tasseling stage, 66 DAP).

Treatment		LAI	CCI	A_n	g_s	RWC
Water Regime (WR)	Nitrogen (N)	($m^2 m^{-2}$)	(r.u.)	($\mu mol m^{-2} s^{-1}$)	($mol m^{-2} s^{-1}$)	(%)
I0	Low	0.6 ± 0.39 c	30.6 ± 9.56 d	0.4 ± 1.01 c	0.01 ± 0.00 c	62.3 ± 2.6 c
	High	0.6 ± 0.07 c	36.9 ± 10.94 c	1.0 ± 1.87 c	0.02 ± 0.00 c	63.8 ± 4.43 bc
I50	Low	2.5 ± 0.5 b	38.9 ± 3.17 c	35.2 ± 8.65 b	0.28 ± 0.10 ab	68.6 ± 14.23 abc
	High	2.8 ± 0.49 ab	49.8 ± 4.2 b	31.9 ± 7.17 b	0.23 ± 0.07 b	74.3 ± 6.18 abc
I100	Low	2.6 ± 0.32 ab	41.1 ± 5.12 c	42.2 ± 3.43 a	0.40 ± 0.08 a	81.0 ± 2.9 ab
	High	3.3 ± 0.69 a	58.9 ± 1.48 a	42.2 ± 1.58 a	0.39 ± 0.05 a	81.6 ± 4.87 a
Water regime		**	*	***	***	**
Nitrogen		ns	***	ns	ns	ns
WR × N		ns	*	ns	ns	ns

ns, *, **, and *** denote not significant or significant at $p \leq 0.05$, 0.01, and 0.001, respectively. Means followed by different letters in each column are significantly different according to the LSD test ($p = 0.05$). Reported values are averages of three replicates.

The highest values of all measured parameters (LAI, CCI, A_n , g_s , and RWC) were observed in the I100 treatment, while the lowest values were recorded for the rainfed (I0) treatment. In comparison to the fully irrigated treatment, LAI decreased by 10% under deficit irrigation and dropped sharply by 80% under rainfed conditions. Leaf gas-exchange parameters exhibited a similar trend: stomatal conductance decreased by 35 and 96% for I50 and I0 treatments, respectively, while net assimilation dropped by 20 and 98%. Conversely, RWC showed minimal changes in both treatments: a decrease of 12% in I50 and 22% in I0. The chlorophyll content index showed a 33% reduction in the average value under rainfed conditions compared to full irrigation. In addition, there was an average decrease of 24% when comparing different nitrogen levels, confirming significant interaction between WR and N.

Correlations among physiological parameters and both RGB and hyperspectral indices, performed on the whole season data, are reported in Figure 2. In the case of RGB indices, the GA index was positively correlated with all variables, especially with LAI, having the strongest correlation (0.79) and T_r (0.75); the lowest correlation was observed for DAGB (0.38). Other indices performed similarly, particularly GGA, NDLab, and ND Luv, but indices b^* and v^* had lower correlation coefficients with the examined variables. In contrast, all parameters had a highly or moderately negative correlation with indices a^* and u^* . As observed for the GA index, all RGB indices showed poor correlation values with DAGB.

No negative correlation was found between narrow-band vegetation indices and physiological variables. The strongest correlation was observed between water indices (WI and WI:NDVI) and REIP with both RWC and canopy temperature (T_c) parameters, with the largest correlation of 0.94 between WI and T_c . High correlation values were also observed between CCI and chlorophyll indices such as MTCl, NDRE, REIP, $CI_{red-edge}$ and the water band index WI. Similarly to RGB indices, all narrow-band indices demonstrated poor correlation with DAGB. Moreover, water indices, especially WI:NDVI, showed a weak

positive correlation with leaf gas-exchange parameters while moderate correlations were recorded for red-edge indices such as NDRE, DD, MTCI and $CI_{red-edge}$.

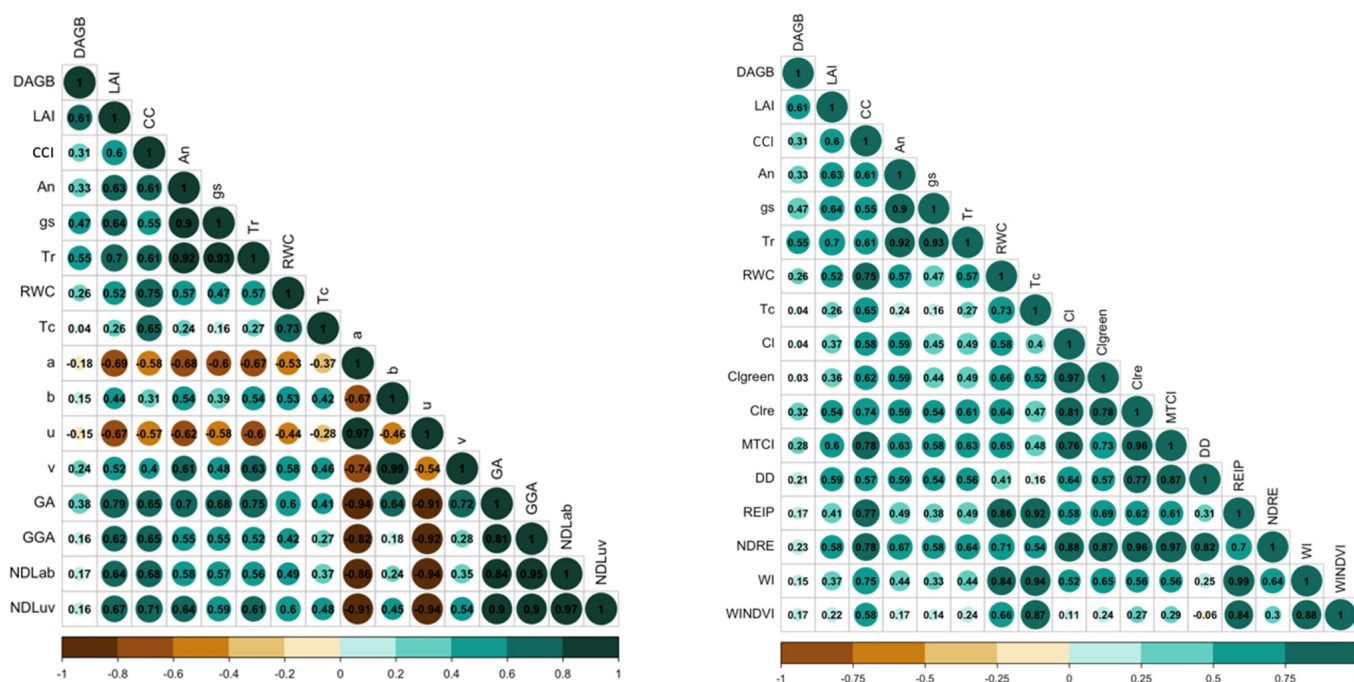


Figure 2. Correlation matrices among sweet maize physiological traits and RGB (left) and hyperspectral (right) indices obtained over the whole growing season.

In our study, the RGB indices (GA, GGA, NDLuv, and NDLab) exhibited strong correlation coefficients with the variables under investigation, greater than those obtained by ground-based hyperspectral indices.

Figure 3 shows the correlation between RGB and hyperspectral indices for the whole growing season. Two RGB indices, a^* and u^* , showed a negative correlation with most of the analyzed indices. Significant negative correlations were observed with the MTCI, DD and NDRE indices. On the contrary, b^* and v^* indices indicated a slight positive correlation with all narrow-band indices, with the largest correlation value with both the REIP and NDRE indices. The GA and GGA indices displayed similar behavior to the normalized NDLab and NDLuv RGB indices. These four indices had significant positive correlation with red-edge vegetation indices, particularly with $CI_{red-edge}$, MTCI, DD and NDRE. Values of correlation with the REIP index were slightly lower. Moreover, the strongest positive correlation with water indices was found between both NDLuv and v^* and WI ($r = 0.55$ and 0.54).

Principal component analysis allowed summarizing the main behaviors observed in the correlation analysis performed on RGB and hyperspectral derived indices. In detail, in the analysis performed on the whole-season data, the first two principal components explained 77.9% of the total variance, with principal component 1 (PC1) and 2 (PC2) accounting for 63.4% and 14.5% of the total variance, respectively (Figure 4).

The inspection of the loadings in the biplot highlighted for PC1 the positive correlation among the four RGB-derived indices, GA, GGA, NDLab and NDLuv, and red-edge vegetation indices $CI_{red-edge}$, MTCI, DD and NDRE, as well as the negative correlation with a^* and u^* . The variable loadings in PC2 highlighted the strong relationship between water band indices (WI and WI:NDVI) and REIP.

In detail, on PC1, the highest weights were observed for NDRE, NDLuv, MTCI, GA, and a*; on PC2, WI:NDVI, WI, REIP, u* and GGA had high weights (Table 4 and Figure 4). Upon inspection of the biplot, it emerged that the scores of the well-watered and fertilized treatments (I100HN) exhibited high positive weights on the first PC, while the rainfed treatments (I0) showed negative scores, both under low and high N levels (LN and HN).

Table 4. Results of the PCA carried out on RGB and hyperspectral indices for the whole growing season of the sweet maize.

Dimension	Eigenvalues	Percentage of Variance	Component Contribution				
			NDRE	NDLuv	MTCI	GA	a*
Dimension 1	11.38	63.40	8.01	7.62	7.58	7.50	7.46
Dimension 2	2.95	14.50	WI:NDVI	WI	REIP	GGA	u*
			18.94	17.54	15.94	9.49	7.31

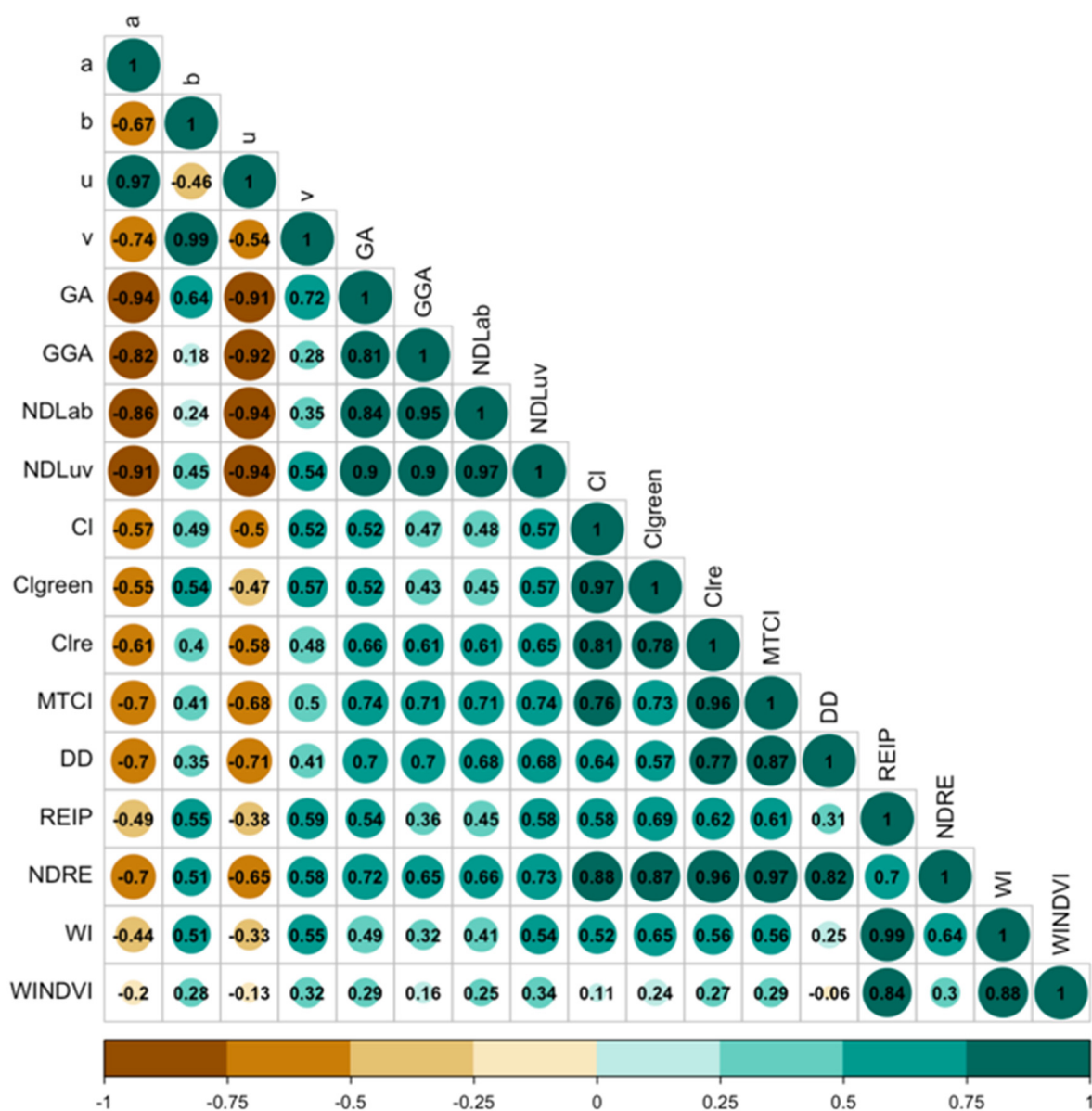


Figure 3. Correlation matrix for the RGB and hyperspectral indices of sweet maize over the whole season.

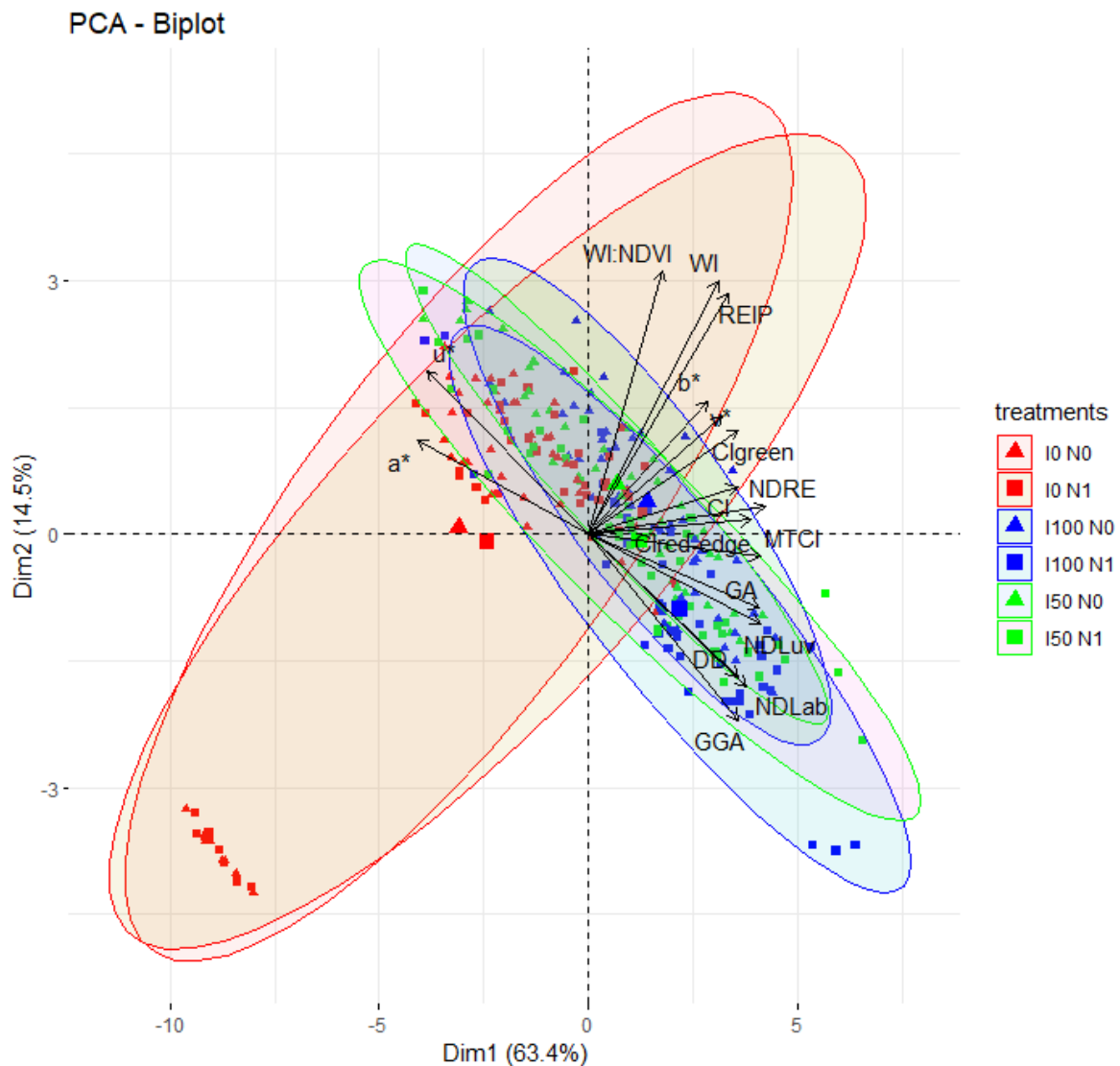


Figure 4. Biplot of the first two principal components (PC1 and PC2), representing component scores (symbols) and variable loadings (vectors), performed for RGB and hyperspectral indices for the whole season.

Concerning the stepwise multilinear regression models (Table 5), the highest R^2 and adjusted R^2 were observed for the model estimating the leaf area index; 63% of the variation in the dependent variable LAI was explained by the change in the independent variables GA, NDLuv and v^* .

Over 60% of chlorophyll content index (CCI) was accounted for by the combination of the same spectral indices (GA and NDLuv), along with b^* and u^* . Notably, the GA index consistently emerged as the primary variable in these models, explaining 61.6% of LAI, 46.1% of stomatal conductance, 56.3% of transpiration rate, and 35.7% of RWC. A prediction model incorporating GA, a^* , and v^* yielded an R^2 of 0.60 for transpiration rate. Additionally, over 55% of RWC was explained by the combination of GA, u^* , and NDLuv. Linear regression equations for DAGB and g_s demonstrated lower adjusted R^2 values of 49 and 47%, respectively, as shown in Table 5. Despite this, all presented models were deemed significant for all physiological parameters.

Table 5. Stepwise multilinear regression models considering the physiological parameters as response variables and RGB-derived indices as predictors.

Variable	Regression Model	R ²	Adjusted R ²	Portion of Variance
LAI	$-1.20 + 6.84 \text{ GA} - 1.38 \text{ NDLuv} - 0.02 \text{ v}^*$	0.637	0.633	GA: 0.616 *** NDLuv: 0.009 v*: 0.012
DAGB	$-999.25 + 4734.94 \text{ GA} + 46.53 \text{ u}^* - 25.50 \text{ b}^* - 1275.89 \text{ NDLuv}$	0.498	0.490	GA: 0.146 *** u*: 0.203 *** b*: 0.091 *** NDLuv: 0.058 ***
CCI	$19.83 + 58.03 \text{ NDLuv} + 1.62 \text{ u}^* + 35.38 \text{ GA} - 0.19 \text{ b}^*$	0.618	0.612	NDLuv: 0.502 *** u*: 0.081 *** GA: 0.026 *** b*: 0.009
A _n	$-19.75 + 0.79 \text{ v}^* + 29.68 \text{ GGA}$	0.535	0.531	v*: 0.374 *** GGA: 0.161 ***
g _s	$-0.12 + 0.63 \text{ GA} + 0.01 \text{ a}^*$	0.474	0.470	GA: 0.461 *** a*: 0.013
T _r	$-3.77 + 13.97 \text{ GA} + 0.19 \text{ a}^* + 0.07 \text{ v}^*$	0.604	0.600	GA: 0.563 *** a*: 0.014 *** v*: 0.024 ***
RWC	$23.45 + 70.49 \text{ GA} + 3.18 \text{ u}^* + 86.87 \text{ NDLuv}$	0.560	0.555	GA: 0.357 *** u*: 0.054 *** NDLuv: 0.149 ***
T _c	$13.43 + 49.77 \text{ NDLuv} + 1.44 \text{ u}^* + 0.30 \text{ v}^*$	0.575	0.570	NDLuv: 0.232 *** u*: 0.255 *** v*: 0.088 ***

*** denotes significant at $p \leq 0.001$.

Stepwise multiple regression analysis conducted with hyperspectral data (see Table 6) revealed that linear regression equations for CCI, RWC, and T_c achieved the highest adjusted R² values, of 74%, 75%, and 82%, respectively. For CCI estimation, the CI_{red-edge} index explained 55.2% of the variance, while WI:NDVI and DD contributed 15.4% and 3.5%, respectively. The water band indices WI and WI:NDVI consistently emerged as main variables in RWC and T_c models, explaining 70% and 77% of variance, respectively. Both g_s and T_r gas exchange parameters were explained by the combination of NDRE and CI indices, despite a low contribution of the latter. In the case of net assimilation rate, 45.7% of its variance was explained by CI_{green}, DD, and WI:NDVI indices. Compared to the results in Table 5, the model for estimating LAI had low R² and an adjusted R² of 0.40. The DAGB model had the lowest R² value among the linear regression equations.

Table 6. Stepwise multilinear regression models considering the physiological parameters as response variables and hyperspectral indices as predictors.

Variable	Regression Model	R ²	Adjusted R ²	Portion of Variance
LAI	$0.08 + 9.38 \text{ DD} + 0.82 \text{ WI:NDVI}$	0.408	0.404	DD: 0.343 *** WI:NDVI: 0.065 ***
DAGB	$207.19 + 3287.9 \text{ CI}_{\text{red-edge}} - 168.11 \text{ CI}$	0.244	0.238	CI _{red-edge} : 0.105 *** CI: 0.139 ***
CCI	$1.5 + 38.5 \text{ CI}_{\text{red-edge}} + 17.14 \text{ WI:NDVI} + 54.21 \text{ DD}$	0.741	0.738	CI _{red-edge} : 0.552 *** WI:NDVI: 0.154 *** DD: 0.035 ***

Table 6. Cont.

Variable	Regression Model	R ²	Adjusted R ²	Portion of Variance
A _n	2.23 + 6.17 CI _{green} + 76.57 DD + 4.22 WI:NDVI	0.457	0.451	CI _{green} : 0.353 *** DD: 0.094 *** WI:NDVI: 0.01
g _s	−0.02 + 1.32NDRE − 0.02CI	0.349	0.346	NDRE: 0.334 *** CI: 0.015
T _r	0.34 + 32.53 NDRE − 0.55 CI	0.435	0.431	NDRE: 0.41 *** CI: 0.025
RWC	0.7 + 69.1 WI + 57.39 DD	0.755	0.752	WI: 0.705 *** DD: 0.05 ***
T _c	2.76 + 16.74 WI:NDVI + 16.63 CI _{red-edge}	0.823	0.821	WI:NDVI: 0.765 *** CI _{red-edge} : 0.058 ***

*** denotes significant at $p \leq 0.001$.

Despite the promising results obtained, it is crucial to recognize the limitations of this approach. These empirical models have not yet been tested on other datasets, necessitating careful consideration.

4. Discussion

4.1. Effect of Water and Nitrogen on the Maize Physiological Parameters

Water stress, associated with high temperatures, is the main cause of limited growth and reduced gas exchanges in maize [51]. In Southern Italy, it often occurs during the tasseling stage (VT), which is one of the phenological stages more sensitive to shortage of water. In fact, the reductions in leaf area and of stomatal conductance are among the first mechanisms to be affected under water deficiency [52]. Nevertheless, in this study, the RWC was much less affected by water stress than other crop parameters, because a strong reduction in stomatal conductance diminished leaf evaporative losses and preserved leaf water status [53].

A significant two-way interaction between water and nitrogen treatment was observed for leaf chlorophyll content index (Table 3). Higher CCI was observed in the well fertilized treatment and within the irrigation treatment. This indicates that (i) water stress impedes the synthesis of chlorophyll, by accelerating its degradation, resulting in a reduced CCI [54], and (ii) a higher application of nitrogen strongly increases CCI [55].

4.2. RGB and Hyperspectral Vegetation Indices for Estimating Maize Physiological Parameters

The vegetation indices obtained from digital RGB imagery have been previously recommended as a means for estimating physiological properties of maize under water- and nitrogen-deficiency conditions [39,42,44].

The results reported in Table 5 indicate that the GA index was selected as the primary variable for predicting several physiological parameters, including leaf area index, transpiration rate, stomatal conductance, and relative water content, because of the strong positive correlation with these indicators. Several authors [39,42] reported the efficacy of GA in estimating vegetation cover due to its capacity to quantify the ratio of green pixels to total pixels in an image.

Kefauver et al. [44] evaluated the use of RGB indices for precise crop management of maize under both fertilizer and irrigation treatments and concluded that GA is an efficient indicator for avoiding background effects (e.g., soil, weeds, etc.), considering only healthy and photosynthetically active vegetation. Therefore, the GA index seems to be more relevant in predicting crop status than other indexes. Our findings, although based on single-year observations, highlight the potentiality of using GA index at the canopy level for enhancing crop management practices of maize and improving crop performance under diverse experimental conditions (water and fertilization inputs).

In our study, the a^* and u^* indices did not carry a high weight in the prediction models. This observation is attributed to the nature of the RGB indices a^* , b^* , u^* , and v^* , which primarily capture the average color of the image, encompassing not only plant pigments but also other visible surfaces like soil and non-photosynthetic vegetation. Specifically, the a^* and u^* indices tend to reflect color components that are highly influenced by the illumination of the scene and adjustments made by the camera, thereby potentially being constrained by variations in soil lightness [56].

Moreover, another aspect to be considered is the spatial resolution. If it is very high, crops in the image are very distinct and separated from disturbance elements (soil, weeds, etc.); vice versa, if the spatial resolution is low, the borders between plants and soil are vague, which implies a higher percentage of pixels containing information from both vegetation and bare soil [57]. Considering the case of the closed canopies, such as occurs in the late maize stages, soil represents a very minimal constituent, as compared to the initial phenological stages; under these conditions, as occurs in our study, the RGB indices are suitable indicators of crop status.

Previous studies comparing the RGB indices and NDVI of maize demonstrated that, although RGB data are affected by a very heterogeneous canopy, they are quite independent from the plant architecture. In fact, the detected visible spectrum is dependent on the pigment's reflectance only of the surface of the photographed canopy [44]. In contrast to RGB indices, NDVI is more disturbed by the sensitivity of the near-infrared reflectance to the canopy architectural changes [58].

The outcomes from the stepwise multilinear regression models employing hyperspectral-derived indices (as depicted in Table 6) underscore the substantial importance (adjusted $R^2 > 0.75$) of both WI and WI:NDVI in forecasting RWC and crop temperature, respectively. These findings align closely with previous studies [59–61] that consistently highlight robust correlation between water band indices and plant water status, particularly in the presence of water stress. The observed correlation between WI and RWC implies a direct connection: as RWC rises, WI also increases, indicating that water stress influences the absorption of water in plant mesophyll pigments. Furthermore, the link between crop water status and WI:NDVI can be attributed to the ability of the NIR wavelengths (specifically at 970 nm) to penetrate deeply into the canopy, thereby enabling the estimation of water content [62,63]. In response to water stress crops close their stomata, resulting in elevated leaf temperatures. This effect can be discerned using water band indices, as observed in our study, and is highlighted by Ihuoma and Madramootoo [64], who reported the efficacy of water band indices in mapping canopy temperature.

Furthermore, the red-edge region demonstrated strong predictive capabilities for gas-exchange parameters. Indices such as $CI_{red-edge}$, NDRE, and DD exhibited promising accuracy in estimating physiological parameters like chlorophyll content [65]. Our study aligns with recent findings that emphasize the sensitivity of red-edge wavelengths to variations in both plant nitrogen and water status.

The potential use of the red-edge region for assessing sweet maize nutritional status was confirmed by a study conducted by [45], who reported that the vegetation indices (NDRE, MTCI and $CI_{red-edge}$), calculated by red-edge wavelengths, were significantly affected by nitrogen levels. As in our study, they pointed out a positive correlation between the red-edge-based VIs and leaf-gas-exchange parameters. DD, REIP, and $CI_{red-edge}$, belonging to the red-edge group VIs, were the best predictors of physiological and yield parameters at the mid-season stage of sweet maize crop. The differences among water supplies and nitrogen treatments are mainly related to chlorophyll content [66].

Moreover, Li et al. [67] noted that NDRE, $CI_{red-edge}$ and other red-edge-derived indices performed similarly to, and constantly better than, some traditional VIs, such as NDVI, in estimating summer maize nitrogen status. This is probably explained by the fact that the red-edge-based VIs can overcome the saturation problems experienced with the NDVI [68–70].

These findings support the growing interest in using carefully chosen narrow-band vegetation indices (VIs) as a non-destructive method for monitoring water and nitrogen levels of sweet maize. Hyperspectral sensors offer continuous measurements, facilitating the detection of subtle surface changes [71]. In particular, red-edge-based indices serve as effective tools for identifying crop deficiencies or assessing nitrogen fertilizer needs [72].

Finally, it is important to mention that the findings of this study are based on one-year experimental data, which might be considered as a limitation in the case of assessing the agronomic performance of a crop under variable climatic conditions. Nevertheless, this study focused on the capability of sensors and aerial RGB and hyperspectral indices to assess the crop's performance under different water and nitrogen inputs. Therefore, the mechanism of response and capability to grasp it through the application of innovative monitoring solutions was investigated, which would not require multi-year and multi-site experimental results.

5. Conclusions

The reliability of aerial-RGB and ground-measured hyperspectral indices to predict sweet maize physiological parameters has been investigated in this study. Among hyperspectral vegetation indices, those based on red-edge wavelengths showed high capability of predicting gas-exchange variables. In addition, stepwise linear regression highlighted the usefulness of both WI and WI:NDVI for relative water-content and crop-temperature prediction. Among RGB indices, GA had the strongest correlation with leaf area index, transpiration rate, stomatal conductance and relative water content. Moreover, the application of GA, GGA, NDLuv and NDLab resulted in high coefficients of correlation with the studied variables, even higher than the hyperspectral indices measured at the ground level. These results support the evidence that vegetation indices derived from RGB images may constitute a particularly cost-effective strategy for crop status monitoring and a more sustainable management of both water and nitrogen inputs.

These results leverage the opportunity of extending the experimentation to a larger number of case studies and scenarios (e.g., growing seasons, other crops, diverse climate, soil and management practices) to better understand the relation between the spectral reflectance captured by both RGB and hyperspectral sensors and the vegetation properties.

Author Contributions: Conceptualization, M.C., R.A., A.M.S., M.T. and V.C.; methodology, M.C., A.M.S. and R.A.; formal analysis and data curation, M.C., N.M., R.A. and A.M.S.; investigation, M.C., M.D.V. and V.C.; writing—original draft preparation, M.C., N.M., R.A., A.M.S., M.D.V., M.T. and V.C.; writing—review and editing, M.C., N.M., R.A., A.M.S., M.D.V., M.T. and V.C.; funding acquisition, M.T. All authors have read and agreed to the published version of the manuscript.

Funding: The research was supported by the Master of Science Program in Water and Land Re-sources Management of CIHEAM Bari (Italy).

Data Availability Statement: Data are contained within the article.

Acknowledgments: The authors thank Carlo Ranieri (CIHEAM Bari) for technical support during the data collection and Mimmo Tribuzio (CIHEAM Bari) for agronomic assistance in the field.

Conflicts of Interest: The authors declare no conflicts of interest.

Abbreviations

Red-green-blue (RGB), red-edge chlorophyll index (Clred-edge), normalized difference red-edge index (NDRE), double difference index (DD), water band index (WI), ratio of water band index and normalized difference vegetation index (WI:NDVI), greener area (GGA), normalized difference between indices u^* and v^* (NDLuv), normalized difference between a^* and b^* (NDLab).

References

- Wik, M.; Pingali, P.; Brocai, S. *Global Agricultural Performance: Past Trends and Future Prospects*; World Bank: Washington, DC, USA, 2008.
- Oliver, M.A.; Bishop, T.F.A.; Marchant, B.P. (Eds.) *Precision Agriculture for Sustainability and Environmental Protection*; Routledge: Abingdon, UK, 2013.
- Liaghat, S.; Balasundram, S.K. A Review: The Role of Remote Sensing in Precision Agriculture. *AJABS* **2010**, *5*, 50–55. [[CrossRef](#)]
- Virnodkar, S.S.; Pachghare, V.K.; Patil, V.C.; Jha, S.K. Remote Sensing and Machine Learning for Crop Water Stress Determination in Various Crops: A Critical Review. *Precis. Agric.* **2020**, *21*, 1121–1155. [[CrossRef](#)]
- Katsoulas, N.; Elvanidi, A.; Ferentinos, K.P.; Kacira, M.; Bartzanas, T.; Kittas, C. Crop Reflectance Monitoring as a Tool for Water Stress Detection in Greenhouses: A Review. *Biosyst. Eng.* **2016**, *151*, 374–398. [[CrossRef](#)]
- Shoshany, M.; Goldshleger, N.; Chudnovsky, A. Monitoring of Agricultural Soil Degradation by Remote-Sensing Methods: A Review. *Int. J. Remote Sens.* **2013**, *34*, 6152–6181. [[CrossRef](#)]
- Xue, J.; Su, B. Significant Remote Sensing Vegetation Indices: A Review of Developments and Applications. *J. Sens.* **2017**, *2017*, 1353691. [[CrossRef](#)]
- Zhang, C.; Kovacs, J.M. The Application of Small Unmanned Aerial Systems for Precision Agriculture: A Review. *Precis. Agric.* **2012**, *13*, 693–712. [[CrossRef](#)]
- Roy, P.S. Spectral Reflectance Characteristics of Vegetation and Their Use in Estimating Productive Potential. *Proc. Plant Sci. J.* **1989**, *99*, 59–81. [[CrossRef](#)]
- Jain, N.; Ray, S.S.; Singh, J.P.; Panigrahy, S. Use of Hyperspectral Data to Assess the Effects of Different Nitrogen Applications on a Potato Crop. *Precis. Agric.* **2007**, *8*, 225–239. [[CrossRef](#)]
- Chappelle, E.W.; Kim, M.S.; McMurtrey, J.E. Ratio Analysis of Reflectance Spectra (RARS): An Algorithm for the Remote Estimation of the Concentrations of Chlorophyll A, Chlorophyll B, and Carotenoids in Soybean Leaves. *Remote Sens. Environ.* **1992**, *39*, 239–247. [[CrossRef](#)]
- Tanriverdi, Ç. A Review of Remote Sensing and Vegetation Indices in Precision Farming. *J. Eng. Sci.* **2006**, *9*, 69–76.
- Pinter, P.J.; Hatfield, J.L.; Schepers, J.S.; Barnes, E.M.; Moran, M.S.; Daughtry, C.S.T.; Upchurch, D.R. Remote Sensing for Crop Management. *Photogramm. Eng. Remote Sens.* **2003**, *69*, 647–664. [[CrossRef](#)]
- Pu, R. Hyperspectral Remote Sensing: Fundamentals and Practices. In *Hyperspectral Remote Sensing: Fundamentals and Practices*; CRC Press: Boca Raton, FL, USA, 2017; pp. 1–466. [[CrossRef](#)]
- Jabbari, E.; Kim, D.H.; Lee, L.P.; Ghaemmaghami, A.; Khademhosseini, A. (Eds.) *Biologically-Driven Engineering of Materials, Processes, Devices, and Systems*. In *Handbook of Biomimetics and Bioinspiration*; World Scientific: Singapore, 2014; pp. 1–1464.
- Main, R.; Cho, M.A.; Mathieu, R.; O’Kennedy, M.M.; Ramoelo, A.; Koch, S. An Investigation into Robust Spectral Indices for Leaf Chlorophyll Estimation. *ISPRS* **2011**, *66*, 751–761. [[CrossRef](#)]
- Thenkabail, P.S.; Lyon, J.G. (Eds.) *Hyperspectral Remote Sensing of Vegetation*. In *Hyperspectral Remote Sensing of Vegetation*, 2nd ed.; Taylor & Francis Group: Boca Raton, FL, USA, 2016.
- Horler, D.N.H.; Dockray, M.; Barber, J. The Red Edge of Plant Leaf Reflectance. *Int. J. Remote Sens.* **1983**, *4*, 273–288. [[CrossRef](#)]
- Schlemmer, M.; Gitelson, A.; Schepers, J.; Ferguson, R.; Peng, Y.; Shanahana, J.; Rundquist, D. Remote Estimation of Nitrogen and Chlorophyll Contents in Maize at Leaf and Canopy Levels. *Int. J. Appl. Earth Obs. Geoinf.* **2013**, *25*, 47–54. [[CrossRef](#)]
- Gao, Y.; Qiu, J.; Miao, Y.; Qiu, R.; Li, H.; Zhang, M. Prediction of Leaf Water Content in Maize Seedlings Based on Hyperspectral Information. *IFAC-PapersOnLine* **2019**, *52*, 263–269. [[CrossRef](#)]
- Elsayed, S.; Darwish, W.; Elsayed, S.; Darwish, W. Hyperspectral Remote Sensing to Assess the Water Status, Biomass, and Yield of Maize Cultivars under Salinity and Water Stress. *Bragantia* **2017**, *76*, 62–72. [[CrossRef](#)]
- Sun, H.; Liu, N.; Wu, L.; Chen, L.; Yang, L.; Li, M.; Zhang, Q. Water Content Detection of Potato Leaves Based on Hyperspectral Image. *IFAC-PapersOnLine* **2018**, *51*, 443–448. [[CrossRef](#)]
- Kovar, M.; Brestic, M.; Sytar, O.; Barek, V.; Hauptvogel, P.; Zivcak, M. Evaluation of Hyperspectral Reflectance Parameters to Assess the Leaf Water Content in Soybean. *Water J.* **2019**, *11*, 443. [[CrossRef](#)]
- Zhao, T.; Nakano, A.; Iwaski, Y.; Umeda, H. Application of Hyperspectral Imaging for Assessment of Tomato Leaf Water Status in Plant Factories. *Appl. Sci.* **2020**, *10*, 4665. [[CrossRef](#)]
- Ranjan, R.; Sahoo, R.N.; Chopra, U.K.; Pramanik, M.; Singh, A.K.; Pradhan, S. Assessment of Water Status in Wheat (*Triticum aestivum* L.) Using Ground Based Hyperspectral Reflectance. *Proc. Natl. Acad. Sci. USA* **2017**, *87*, 377–388. [[CrossRef](#)]
- Penuelas, J.; Pinol, J.; Ogaya, R.; Filella, I. Estimation of Plant Water Concentration by the Reflectance Water Index WI (R900/R970). *Int. J. Remote Sens.* **1997**, *18*, 2869–2875. [[CrossRef](#)]
- Hunt, E.R.; Rock, B.N. Detection of Changes in Leaf Water Content Using Near- and Middle-Infrared Reflectances. *Remote Sens. Environ.* **1989**, *30*, 43–54. [[CrossRef](#)]
- Prasad, B.; Carver, B.F.; Stone, M.L.; Babar, M.A.; Raun, W.R.; Klatt, A.R. Potential Use of Spectral Reflectance Indices as a Selection Tool for Grain Yield in Winter Wheat under Great Plains Conditions. *Crop. Sci.* **2007**, *47*, 1426–1440. [[CrossRef](#)]
- Zarco-Tejada, P.J.; Rueda, C.A.; Ustin, S.L. Water Content Estimation in Vegetation with MODIS Reflectance Data and Model Inversion Methods. *Remote Sens. Environ.* **2003**, *85*, 109–124. [[CrossRef](#)]
- Wachendorf, M.; Fricke, T.; Möckel, T. Remote Sensing as a Tool to Assess Botanical Composition, Structure, Quantity and Quality of Temperate Grasslands. *Grass Forage Sci.* **2018**, *73*, 1–14. [[CrossRef](#)]

31. Mulla, D.J. Twenty Five Years of Remote Sensing in Precision Agriculture: Key Advances and Remaining Knowledge Gaps. *Biosyst. Eng.* **2013**, *114*, 358–371. [[CrossRef](#)]
32. Danzi, D.; Briglia, N.; Petrozza, A.; Summerer, S.; Povero, G.; Stivaletta, A.; Cellini, F.; Pignone, D.; de Paola, D.; Janni, M. Can High Throughput Phenotyping Help Food Security in the Mediterranean Area? *Front. Plant Sci.* **2019**, *10*, 433452. [[CrossRef](#)]
33. Tsouros, D.C.; Bibi, S.; Sarigiannidis, P.G. A Review on UAV-Based Applications for Precision Agriculture. *Information* **2019**, *10*, 349. [[CrossRef](#)]
34. Yadav, S.P.; Ibaraki, Y.; Gupta, S.D. Estimation of the Chlorophyll Content of Micropropagated Potato Plants Using RGB Based Image Analysis. *Plant Cell Tissue Organ Cult.* **2010**, *100*, 183–188. [[CrossRef](#)]
35. Yousfi, S.; Gracia-Romero, A.; Kellas, N.; Kaddour, M.; Chadouli, A.; Karrou, M.; Araus, J.L.; Serret, M.D. Combined Use of Low-Cost Remote Sensing Techniques and $\Delta^{13}C$ to Assess Bread Wheat Grain Yield under Different Water and Nitrogen Conditions. *Agronomy* **2019**, *9*, 285. [[CrossRef](#)]
36. Sankaran, S.; Khot, L.R.; Espinoza, C.Z.; Jarolmasjed, S.; Sathuvalli, V.R.; Vandemark, G.J.; Miklas, P.N.; Carter, A.H.; Pumphrey, M.O.; Knowles, R.R.N.; et al. Low-Altitude, High-Resolution Aerial Imaging Systems for Row and Field Crop Phenotyping: A Review. *Eur. J. Agron.* **2015**, *70*, 112–123. [[CrossRef](#)]
37. Norasma, C.Y.N.; Abu Sari, M.Y.; Fadzilah, M.A.; Ismail, M.R.; Omar, M.H.; Zulkarami, B.; Hassim, Y.M.M.; Tarmidi, Z. Rice Crop Monitoring Using Multicopter UAV and RGB Digital Camera at Early Stage of Growth. *IOP Conf. Ser. Earth Environ. Sci.* **2018**, *169*, 012095. [[CrossRef](#)]
38. Fernandez-Gallego, J.A.; Kefauver, S.C.; Vatter, T.; Aparicio Gutiérrez, N.; Nieto-Taladriz, M.T.; Araus, J.L. Low-Cost Assessment of Grain Yield in Durum Wheat Using RGB Images. *Eur. J. Agron.* **2019**, *105*, 146–156. [[CrossRef](#)]
39. Buchaillet, M.L.; Gracia-Romero, A.; Vergara-Díaz, O.; Zaman-Allah, M.A.; Tareknege, A.; Cairns, J.E.; Prasanna, B.M.; Araus, J.L.; Kefauver, S.C. Evaluating Maize Genotype Performance under Low Nitrogen Conditions Using RGB UAV Phenotyping Techniques. *Sensors* **2019**, *19*, 1815. [[CrossRef](#)]
40. Wakabayashi, H.; Matsuda, O.; Fujita, T.; Kume, A. Practical Application of Proximal Sensing for Monitoring the Growth of Physcomitrium Patens. *Biol. Sci. Space* **2021**, *35*, 32–40. [[CrossRef](#)]
41. Purcell, L.C.; Mozaffari, M.; Karcher, D.E.; Andy King, C.; Marsh, M.C.; Longer, D.E. Association of “Greenness” in Corn with Yield and Leaf Nitrogen Concentration. *Agron. J.* **2011**, *103*, 529–535. [[CrossRef](#)]
42. Gracia-Romero, A.; Kefauver, S.C.; Vergara-Díaz, O.; Zaman-Allah, M.A.; Prasanna, B.M.; Cairns, J.E.; Araus, J.L. Comparative Performance of Ground vs. Aerially Assessed Rgb and Multispectral Indices for Early-Growth Evaluation of Maize Performance under Phosphorus Fertilization. *Front. Plant Sci.* **2017**, *8*, 309121. [[CrossRef](#)]
43. Casadesús, J.; Kaya, Y.; Bort, J.; Nachit, M.M.; Araus, J.L.; Amor, S.; Ferrazzano, G.; Maalouf, F.; Maccaferri, M.; Martos, V.; et al. Using Vegetation Indices Derived from Conventional Digital Cameras as Selection Criteria for Wheat Breeding in Water-Limited Environments. *Ann. Appl. Biol.* **2007**, *150*, 227–236. [[CrossRef](#)]
44. Kefauver, S.C.; El-Haddad, G.; Vergara-Díaz, O.; Araus, J.L. RGB Picture Vegetation Indexes for High-Throughput Phenotyping Platforms (HTPPs). In Proceedings of the Remote Sensing for Agriculture, Ecosystems, and Hydrology XVII, Toulouse, France, 14 October 2015.
45. Colovic, M.; Yu, K.; Todorovic, M.; Cantore, V.; Hamze, M.; Albrizio, R.; Stellacci, A.M. Hyperspectral Vegetation Indices to Assess Water and Nitrogen Status of Sweet Maize Crop. *Agronomy* **2022**, *12*, 2181. [[CrossRef](#)]
46. Allen, R.G.; Pereira, L.S.; Raes, D.; Smith, M. *Crop Evapotranspiration. Guidelines for Computing Crop Water Requirements*; Irrigation and Drainage Paper 56; Food and Agriculture Organization: Rome, Italy, 1998.
47. Trussell, H.J.; Lin, J.; Shamey, R. Effects of Texture on Color Perception. In Proceedings of the 2011 IEEE 10th IVMSWP Workshop: Perception and Visual Signal Analysis, Ithaca, NY, USA, 16 June 2011.
48. Shiratsuchi, L.; Ferguson, R.; Shanahan, J.; Adamchuk, V.; Rundquist, D.; Marx, D.; Slater, G.; Shiratsuchi, L.; Ferguson, R. Water and Nitrogen Effects on Active Canopy Sensor Vegetation Indices. *Agron. J.* **2011**, *103*, 1815–1826. [[CrossRef](#)]
49. Vogelmann, J.E.; Rock, B.N.; Moss, D.M. Red Edge Spectral Measurements from Sugar Maple Leaves. *Remote Sens.* **1993**, *14*, 1563–1575. [[CrossRef](#)]
50. Barnes, E.; Clarke, T.; Richards, S.; Colaizzi, P.; Haberland, J.; Kostrzewski, M.; Waller, P.; Choi, C.; Riley, E.; Thompson, T.; et al. Coincident Detection of Crop Water Stress, Nitrogen Status and Canopy Density Using Ground-Based Multispectral Data. In Proceedings of the 5th International Conference on Precision Agriculture, Bloomington, MN, USA, 16–19 July 2000.
51. Hu, J.; Zhao, X.; Gu, L.; Liu, P.; Zhao, B.; Zhang, J.; Ren, B. The Effects of High Temperature, Drought, and Their Combined Stresses on the Photosynthesis and Senescence of Summer Maize. *Agric. Water Manag.* **2023**, *289*, 108525. [[CrossRef](#)]
52. Hsiao, T.C. Plant Responses to Water Stress. *Annu. Rev. Plant Physiol.* **2003**, *24*, 519–570. [[CrossRef](#)]
53. Bennett, J.M.; Sinclair, T.R.; Muchow, R.C.; Costello, S.R. Dependence of Stomatal Conductance on Leaf Water Potential, Turgor Potential, and Relative Water Content in Field-Grown Soybean and Maize. *Crop. Sci.* **1987**, *27*, 984–990. [[CrossRef](#)]
54. Mihailović, N.; Jelić, G.; Filipović, R.; Djurdjević, M.; Dželetović, Z. Effect of Nitrogen Form on Maize Response to Drought Stress. *Plant Soil* **1992**, *144*, 191–197. [[CrossRef](#)]
55. Adrienn, V.S.; Janos, N. Effects of Nutrition and Water Supply on the Yield and Grain Protein Content of Maize Hybrids. *Aust. J. Crop Sci.* **2012**, *6*, 381–390.
56. Casadesús, J.; Villegas, D. Conventional Digital Cameras as a Tool for Assessing Leaf Area Index and Biomass for Cereal Breeding. *J. Integr. Plant Biol.* **2014**, *56*, 7–14. [[CrossRef](#)] [[PubMed](#)]

57. Torres-Sánchez, J.; Peña, J.M.; de Castro, A.I.; López-Granados, F. Multi-Temporal Mapping of the Vegetation Fraction in Early-Season Wheat Fields Using Images from UAV. *Comput. Electron. Agric.* **2014**, *103*, 104–113. [[CrossRef](#)]
58. Gitelson, A.A.; Stark, R.; Grits, U.; Rundquist, D.; Kaufman, Y.; Derry, D. Vegetation and Soil Lines in Visible Spectral Space: A Concept and Technique for Remote Estimation of Vegetation Fraction. *Int. J. Remote Sens.* **2002**, *23*, 2537–2562. [[CrossRef](#)]
59. El-Hendawy, S.; Al-Suhaibani, N.; Salem, A.E.A.; Ur Rehman, S.; Schmidhalter, U. Spectral Reflectance Indices as a Rapid and Nondestructive Phenotyping Tool for Estimating Different Morphophysiological Traits of Contrasting Spring Wheat Germplasms under Arid Conditions. *Turk. J. Agric. For.* **2015**, *39*, 572–587. [[CrossRef](#)]
60. Peñuelas, J.; Inoue, Y. Reflectance Indices Indicative of Changes in Water and Pigment Contents of Peanut and Wheat Leaves. *Photosynthetica* **1999**, *36*, 355–360. [[CrossRef](#)]
61. Penuelas, J.; Filella, I.; Biel, C.; Serrano, L.; Save, R. The Reflectance at the 950–970 Nm Region as an Indicator of Plant Water Status. *Int. J. Remote Sens.* **1993**, *14*, 1887–1905. [[CrossRef](#)]
62. Gutierrez, M.; Reynolds, M.P.; Raun, W.R.; Stone, M.L.; Klatt, A.R. Spectral Water Indices for Assessing Yield in Elite Bread Wheat Genotypes under Well-Irrigated, Water-Stressed, and High-Temperature Conditions. *Crop. Sci.* **2010**, *50*, 197–214. [[CrossRef](#)]
63. Babar, M.A.; Reynolds, M.P.; Van Ginkel, M.; Klatt, A.R.; Raun, W.R.; Stone, M.L. Spectral Reflectance to Estimate Genetic Variation for In-Season Biomass, Leaf Chlorophyll, and Canopy Temperature in Wheat. *Crop. Sci.* **2006**, *46*, 1046–1057. [[CrossRef](#)]
64. Ihuoma, S.O.; Madramootoo, C.A. Narrow-Band Reflectance Indices for Mapping the Combined Effects of Water and Nitrogen Stress in Field Grown Tomato Crops. *Biosyst. Eng.* **2020**, *192*, 133–143. [[CrossRef](#)]
65. Elmetwalli, A.H.; Tyler, A.N. Estimation of Maize Properties and Differentiating Moisture and Nitrogen Deficiency Stress via Ground-Based Remotely Sensed Data. *Agric. Water Manag.* **2020**, *242*, 106413. [[CrossRef](#)]
66. Sellami, M.H.; Albrizio, R.; Čolović, M.; Hamze, M.; Cantore, V.; Todorovic, M.; Piscitelli, L.; Stellacci, A.M. Selection of Hyperspectral Vegetation Indices for Monitoring Yield and Physiological Response in Sweet Maize under Different Water and Nitrogen Availability. *Agronomy* **2022**, *12*, 489. [[CrossRef](#)]
67. Li, F.; Miao, Y.; Feng, G.; Yuan, F.; Yue, S.; Gao, X.; Liu, Y.; Liu, B.; Ustin, S.L.; Chen, X. Improving Estimation of Summer Maize Nitrogen Status with Red Edge-Based Spectral Vegetation Indices. *Field Crop. Res.* **2014**, *157*, 111–123. [[CrossRef](#)]
68. Kanke, Y.; Raun, W.; Solie, J.; Stone, M.; Taylor, R. Red edge as a potential index for detecting differences in plant nitrogen status in winter wheat. *J. Plant Nutr.* **2012**, *35*, 1526–1541. [[CrossRef](#)]
69. Nguy-Robertson, A.; Gitelson, A.; Peng, Y.; Viña, A.; Arkebauer, T.; Rundquist, D.; Nguy-Robertson, A.; Gitelson, A.; Peng, Y.; Rundquist, D.; et al. Green Leaf Area Index Estimation in Maize and Soybean: Combining Vegetation Indices to Achieve Maximal Sensitivity. *Agron. J.* **2012**, *104*, 1336–1347. [[CrossRef](#)]
70. Van Niel, T.G.; McVicar, T.R. Current and Potential Uses of Optical Remote Sensing in Rice-Based Irrigation Systems: A Review. *Aust. J. Agric. Res.* **2004**, *55*, 155–185. [[CrossRef](#)]
71. Jones, H.G.; Vaughan, R.A. Remote Sensing of Vegetation: Principles, Techniques and Applications. *J. Veg. Sci.* **2011**, *22*, 1151–1153.
72. Raper, T.B.; Varco, J.J. Canopy-Scale Wavelength and Vegetative Index Sensitivities to Cotton Growth Parameters and Nitrogen Status. *Precis. Agric.* **2014**, *16*, 62–76. [[CrossRef](#)]

Disclaimer/Publisher’s Note: The statements, opinions and data contained in all publications are solely those of the individual author(s) and contributor(s) and not of MDPI and/or the editor(s). MDPI and/or the editor(s) disclaim responsibility for any injury to people or property resulting from any ideas, methods, instructions or products referred to in the content.